Direct experimental evidence of a growing length scale accompanying the glass transition

L. Berthier,[1] G. Biroli,[2] J.-P. Bouchaud,[3,4] L. Cipelletti,[1] D. El Masri,[1] D. L'Hôte,[3] F. Ladieu,[3] and M. Pierno[1]

[1]*Laboratoire des Colloïdes, Verres et Nanomatériaux UMR 5587,*
Université Montpellier II and CNRS, 34095 Montpellier, France
[2]*Service de Physique Théorique Orme des Merisiers – CEA Saclay, 91191 Gif sur Yvette Cedex, France*
[3]*Service de Physique de l'État Condensé Orme des Merisiers – CEA Saclay, 91191 Gif sur Yvette Cedex, France*
[4]*Science & Finance, Capital Fund Management 6-8 Bd Haussmann, 75009 Paris, France*
(Dated: November 2, 2018)

Understanding glass formation is a challenge because the existence of a true glass state, distinct from liquid and solid, remains elusive: Glasses are liquids that have become too viscous to flow. An old idea, as yet unproven experimentally, is that the dynamics becomes sluggish as the glass transition approaches because increasingly larger regions of the material have to move simultaneously to allow flow. We introduce new multipoint dynamical susceptibilities to estimate quantitatively the size of these regions and provide direct experimental evidence that the glass formation of molecular liquids and colloidal suspensions is accompanied by growing dynamic correlation length scales.

Why does the viscosity of glass-forming liquids increase so dramatically when approaching the glass transition? Despite decades of research a clear explanation of this phenomenon, common to materials as diverse as molecular glasses, polymers, and colloids is still lacking [1, 2]. The conundrum is that the static structure of a glass is indistinguishable from that of the corresponding liquid, with no sign of increasing static correlation length scales accompanying the glass transition. Numerical simulations performed well above the glass temperature, T_g, reveal instead the existence of a growing dynamic length scale [3, 4, 5, 6, 7] associated to dynamic heterogeneities [8]. Experiments [8, 9, 10, 11, 12] have indirectly suggested a characteristic length scale of about 5 to 20 molecular diameters at T_g, but its time and temperature dependencies, which are crucial for relating this finding to the glass transition, were not determined.

We present quantitative experimental evidence that glass formation in molecular liquids and colloids is accompanied by at least one growing dynamic length scale. We introduce experimentally accessible multipoint dynamic susceptibilities that quantify the correlated nature of the dynamics in glass formers. Because these measurements can be made using a wide variety of techniques in vastly different materials, a detailed characterization of the microscopic mechanisms governing the formation of amorphous glassy states becomes possible.

Supercooled liquids are believed to exhibit spatially heterogeneous dynamics over length scales that grow when approaching the glass state [1, 13, 14, 15]. This heterogeneity implies the existence of significant fluctuations of the dynamics because the number of independently relaxing regions is reduced. Numerical simulations have focused on a "four-point" dynamic susceptibility $\chi_4(t)$, which quantifies the amplitude of spontaneous fluctuations around the average dynamics [3, 4, 5, 6, 7]. The latter is usually measured through ensemble-averaged correlators, $F(t) = \langle \delta A(t)\delta A(0)\rangle = \langle C(t)\rangle$, where $\delta A(t) = $ $A(t) - \langle A \rangle$ represents the spontaneous fluctuation of an observable $A(t)$, such as the density. Dynamic correlation leads to large fluctuations of $C(t)$, measured by $\chi_4(t) = N\langle \delta C^2(t)\rangle$, where N is the number of particles in the system. The susceptibility $\chi_4(t)$ typically presents a nonmonotonic time dependence with a peak centered at the liquid's relaxation time [16]. The height of this peak is proportional to the volume within which correlated motion takes place [4, 5, 15, 16]. Unfortunately, numerical findings are limited to short timescales ($\sim 10^{-7}$ s) and temperatures far above T_g. Experimentally, detecting spontaneous fluctuations of dynamic correlators remains an open challenge, because dynamic measurements have to be resolved in both space and time [17].

Induced fluctuations are more easily accessible experimentally than spontaneous ones and can be related to one another by fluctuation-dissipation theorems. We introduce a dynamic susceptibility defined as the response of the correlator $F(t)$ to a perturbing field x:

$$\chi_x(t) = \frac{\partial F(t)}{\partial x} \tag{1}$$

The relaxation time of supercooled liquids increases abruptly upon cooling, so a relevant perturbing field is temperature, in which case Eq. 1 becomes $\chi_T(t) = \partial F(t)/\partial T$. Density also plays a role in supercooled liquids, although a less crucial one [18]. Hence, another interesting susceptibility is $\chi_P(t) = \partial F(t)/\partial P$, where P is the pressure. Colloidal hard spheres undergo a glass transition [19] at high particle volume fraction φ. Thus, the appropriate susceptibility for colloids is $\chi_\varphi(t) = \partial F(t)/\partial \varphi$. Equation 1 also applies in the frequency domain, $\chi_x(\omega) = \partial \tilde{F}(\omega)/\partial x$, where $\tilde{F}(\omega)$ can be the dielectric susceptibility. We will show below that linear response formalism and fluctuation theory can be used to relate $\chi_x(t)$ to the spontaneous fluctuations of $C(t)$, and thus to $\chi_4(t)$. Thus, $\chi_x(t)$ is an experimentally accessible multi-point dynamic susceptibility that

directly quantifies dynamic heterogeneity in glass formers.

For molecular liquids, the dynamics conserves energy, volume and number N of particles, and one can establish, in the NPT ensemble relevant for experiments, the following fluctuation-dissipation theorem,

$$k_B T^2 \chi_T(t) = N \langle \delta C(t) \delta H(0) \rangle \qquad (2)$$

where k_B is the Boltzmann constant, $H(t)$ the fluctuating enthalpy per particle, and $C(t)$ the instantaneous value of a generic dynamic correlator $F(t)$. Both $C(t)$ and $H(t)$ are sums over local contributions [20], $NC(t) = \rho \int d^3\vec{r} c(\vec{r}, t)$ and $NH(t) = \rho\sqrt{k_B c_P} T \int d^3\vec{r} \hat{h}(\vec{r}, t)$. Here, ρ is the average number density, c_P the constant pressure specific heat that sets the scale of the enthalpy fluctuations, $\langle \delta H^2 \rangle = k_B c_P T^2$, so that the field $\hat{h}(\vec{r}, t)$ has unit variance. Using translational invariance, Eq. 2 can be rewritten as:

$$\sqrt{\frac{k_B}{c_P}} T \chi_T(t) = \rho \int d^3\vec{r} \left\langle \delta c(\vec{r}, t) \delta \hat{h}(\vec{0}, 0) \right\rangle \qquad (3)$$

This expression shows that $\chi_T(t)$ directly probes the range of spatial correlations between local fluctuations of the dynamics and that of the enthalpy. In the case of colloids, the dynamics only conserves density and a similar expression can be obtained

$$\sqrt{\rho k_B T \kappa_T} \, \varphi \chi_\varphi(t) = \rho \int d^3\vec{r} \left\langle \delta c(\vec{r}, t) \delta \hat{\rho}(\vec{0}, 0) \right\rangle \qquad (4)$$

where κ_T is the isothermal compressibility and $\delta\hat{\rho}$ denotes density fluctuations rescaled by their root mean square.

Equations 3 and 4 show that $\chi_x(t)$ probes the extent of spatial dynamic correlations that differ from the ones studied in earlier theoretical and numerical works, which focused instead on $\chi_4(t) = \rho \int d^3\vec{r} \langle \delta c(\vec{r}, t) \delta c(\vec{0}, t) \rangle$. We have, however, established a direct relation between $\chi_x(t)$ and $\chi_4(t)$ by using the thermodynamic formalism developed in [21], which is generically applicable to bulk glass formers above the glass transition. For dynamics conserving energy and volume, we relate the fluctuations of $C(t)$, and therefore $\chi_4(t)$ measured in the NPT ensemble, to its isobaric-isoenthalpic counterpart, $\chi_4^{NPH}(t)$, which quantifies the amplitude of the fluctuations of $C(t)$ in the NPH ensemble in which all configurations have exactly the same enthalpy: $\chi_4(t) = \chi_4^{NPH}(t) + k_B T^2 \chi_T^2(t)/c_P$. Because $\chi_4^{NPH}(t) > 0$, one derives an experimentally measurable rigorous lower bound [22] for $\chi_4(t)$:

$$\chi_4(t) \geq \frac{k_B}{c_P} T^2 \chi_T^2(t) \qquad (5)$$

A similar inequality holds between $\chi_4(\omega)$ and $\chi_T(\omega)$, where $\chi_4(\omega)$ denotes the amplitude of spontaneous fluctuations around $\tilde{F}(\omega)$. Similar arguments also apply to $\chi_4(t)$ computed in the NVT ensemble preferred in numerical simulations. In that case, energy replaces enthalpy in Eqs. 2 and 3, and the specific heat at constant volume, c_V, replaces c_P in Eq. 3 and relation 5. Finally, we find that an inequality similar to relation 5 holds for colloidal systems, for which the volume and the number of particles are conserved quantities:

$$\chi_4(t) \geq \rho k_B T \kappa_T \, \varphi^2 \chi_\varphi^2(t) \qquad (6)$$

We have determined $\chi_x(t)$ experimentally and numerically in three representative glass formers. For supercooled glycerol near $T_g \approx 185$ K, the real part of the dielectric susceptibility, $\epsilon'(\omega)$, was measured every 1 K in the temperature range from 192 K to 232 K. After fitting to a Havriliak-Negami form [1], we use smoothed finite differences to evaluate $\chi_T(\omega) = \partial[\epsilon'(\omega)/\epsilon'(0)]/\partial T$ and show in Fig. 1A the right hand side of relation 5 as a function of inverse frequency. We plot in Fig. 1B the right side of relation 6 for hard sphere colloids where $\chi_\varphi(t) = \partial f(q, t)/\partial\varphi$. The normalized intermediate scattering function [20] $f(q, t)$ is measured by dynamic light scattering [23] for a wavevector q close to the first peak of the static structure factor. Several packing fractions are studied, from diluted samples where $f(q, t)$ decays exponentially in ~ 1 ms to concentrated suspensions with a two-step decay and a final relaxation time of ~ 10 s. Finite differences of data sets obtained for nearby φ are used to deduce $\chi_\varphi(t)$. Finally, we show in Fig. 1C numerical data obtained by standard molecular dynamics simulations of a binary Lennard-Jones mixture, a well-studied model for fragile supercooled liquids [24, 25]. The dynamics is recorded at nearby temperatures through the self part of the intermediate scattering function, whose characteristic decay time spans a range from 1 ps to 100 ns (using Argon units [24, 25]).

Dynamical susceptibilities behave similarly in all three cases. All display a peak for $t \approx \tau_\alpha$, the average relaxation time. The peak height increases when the glass transition is approached. This behavior represents the central result of our work. Together with Eqs. 3 to 6, it provides direct evidence of enhanced dynamic fluctuations and a growing dynamic lengthscale associated with the glass transition.

How tight the bounds of relations 5 and 6 are depends upon the specific material and range of parameters studied. A quantitative answer is given by simulations where the microcanonical quantity $\chi_4^{\text{micro}}(t)$, i.e. the difference between $\chi_4(t)$ in the NVT ensemble and $k_B T^2 \chi_T(t)/c_V$, can be easily measured. For the Lennard-Jones mixture, we find that the right side of relation 5 is much smaller than $\chi_4(t)$ at high T, but the difference rapidly diminishes when T decreases. Both sides of relation 5 become comparable for the lowest temperature shown in Fig. 1C, which is still well above T_g. Following Ref. [26], we also find that mode-coupling theory predicts $\chi_4(t) \sim \chi_T^2(t) \sim (T/T_c - 1)^{-2}$ near the mode-coupling singularity $T_c > T_g$, provided that conserved variables are properly taken into account.

These results support the idea that relation 5 can be used as an equality to quantitatively estimate $\chi_4(t)$ at low temperature, at least for fragile systems. This use
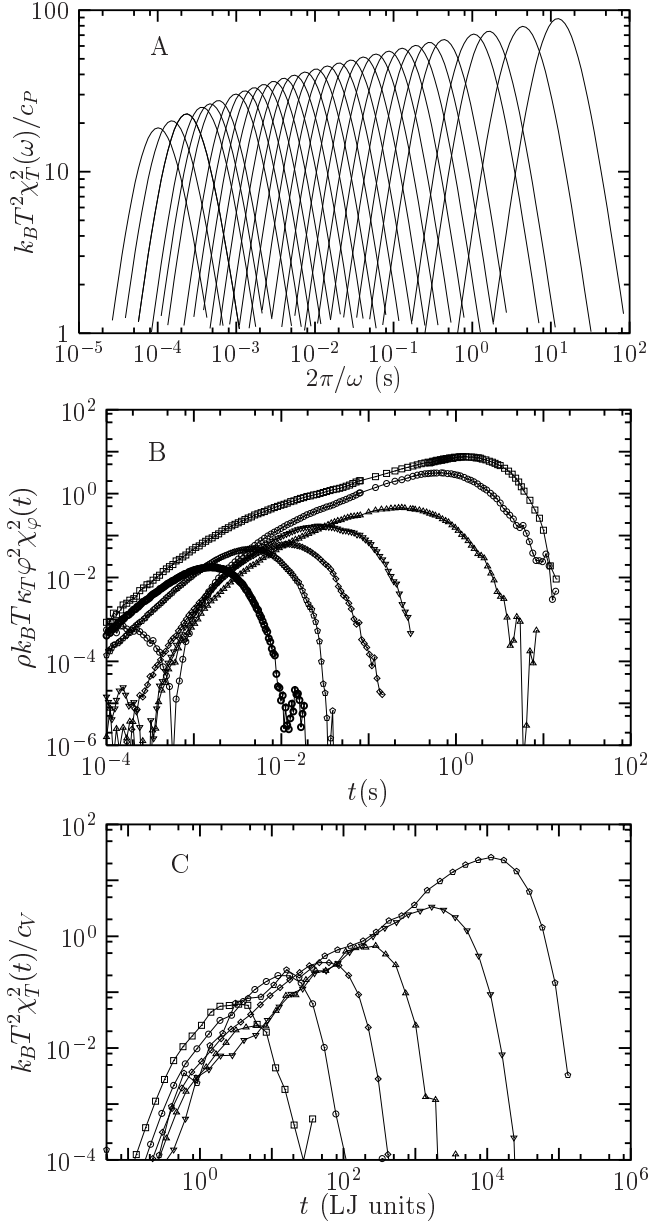
FIG. 1: Dynamic susceptibilities in "χ_4 units", right side of relations 5 and 6 for three glass-formers. (A) $\chi_T(\omega)$ was obtained for 99.6% pure supercooled glycerol (in a desiccated Argon environment to prevent water absorption) by using standard capacitive dielectric measurements for 192 K $\leq T \leq$ 232 K ($T_g \approx 185$ K). (B) $\chi_\varphi(t)$ was obtained in colloidal hard spheres via dynamic light scattering. The static prefactor, $\rho k_B T \kappa_T$, was evaluated from the Carnahan-Starling equation of state [20]. From left to right, $\varphi = 0.18, 0.34, 0.42, 0.46,$ 0.49, and 0.50. (C) $\chi_T(t)$ was obtained in a binary Lennard-Jones (LJ) mixture via numerical simulations. From left to right, $T = 2.0, 1.0, 0.74, 0.6, 0.5$ and 0.465 (in reduced LJ units [24, 25]). Relative errors at the peak are at most about 10% for (A) and (C), and 30% for (B). For all of the systems, dynamic susceptibilities display a peak at the average relaxation time whose height increases when the dynamics slows down, which is direct evidence of enhanced dynamic fluctuations and a growing dynamic length scale.

of relation 5 is equivalent to assuming that dynamic heterogeneity in molecular liquids is strongly correlated with enthalpy fluctuations, and through a similar argument, with density fluctuations in colloids. In fact, supposing that enthalpy is the only source of fluctuations, $\delta C \approx (\partial C/\partial T)_P \delta H/c_P$, and if we use the definition of c_P, we obtain directly that $\chi_4(t) \approx k_B T^2 \chi_T^2(t)/c_P$. A more general result can be obtained by taking into account that energy and density are both fluctuating quantities, in which case $\chi_4(t)$ is the sum of two contributions: $\chi_4(t) \approx k_B T^2 \chi_T^2(t)/c_V + \rho k_B T \kappa_T \rho^2 \chi_\rho^2(t)$. The second term is negligible in most fragile liquids [18], but dominates in colloidal systems. The presence of additional sources of fluctuations justifies that the rigorously derived inequality 5 does not hold as an equality.

Our results for dynamic fluctuations provide an estimate of the size ξ of dynamic heterogeneity in liquids near T_g. Because $\chi_4(t) = \rho \int d^3\vec{r}\langle\delta c(\vec{r},t)\delta c(\vec{0},t)\rangle$, this quantity, once divided by the amplitude of the fluctuations at zero distance, $\langle\delta c^2(\vec{0},t)\rangle$, defines a correlation volume. The correlation functions are normalized to unity at $t = 0$, so $\langle\delta c^2(\vec{0},t)\rangle$ is of order one or smaller. Our simulations indeed show that in the temperature regime where the dynamics slows down and on timescales not much longer than the system relaxation time, this average is of the order of one and displays extremely weak temperature dependence, as expected for a local quantity in glass formers. Thus, the height of the peak in the dynamic susceptibility, $\chi_4^\star \approx k_B T^2 (\chi_T^\star)^2/c_P$, yields directly a correlation volume expressed in molecular units, $\chi_4^\star \simeq (\xi/a)^\zeta$, where a is the molecular size and c_P is expressed in units of k_B. Numerical [4, 6] and theoretical [6, 15, 16, 26] works suggest that $\zeta \approx 2$ to 4.

A direct comparison between our data and existing measurements can be performed for glycerol, where multidimensional nuclear magnetic resonance (NMR) experiments show that $\xi = 1.3\pm0.5$ nm for $T = 199$ K [27, 28]. Assuming a simple compact geometry for heterogeneities, $\zeta = 3$, we estimate that ξ increases from 0.9 nm at $T = 232$ K to 1.5 nm at 192 K. Given the assumptions involved in both approaches, and the uncertainty about numerical prefactors of order unity, the agreement is remarkable. An important physical conclusion of our work is that dynamic heterogeneity is strongly correlated to enthalpy fluctuations in fragile liquids, although there is no signature of any static large-scale correlations [3, 6, 15].

For other glass-forming liquids, we obtain an estimate for ξ at T_g by assuming for simplicity that correlators obey time-temperature superposition, $F(t) = \mathcal{F}(t/\tau_\alpha)$, and using relation 5 as an equality. One gets

$$\chi_4^\star(T_g) \approx [\mathcal{F}'(1)]^2 \frac{k_B}{c_P}\left(\frac{\partial \ln \tau_\alpha}{\partial \ln T}\Big|_{T_g}\right)^2 \qquad (7)$$

The logarithmic derivative is proportional to the well-known "steepness index" m, introduced in the glass literature to characterize the fragility of glass-forming liquids [29]. From reported values [1, 29] of the quantities
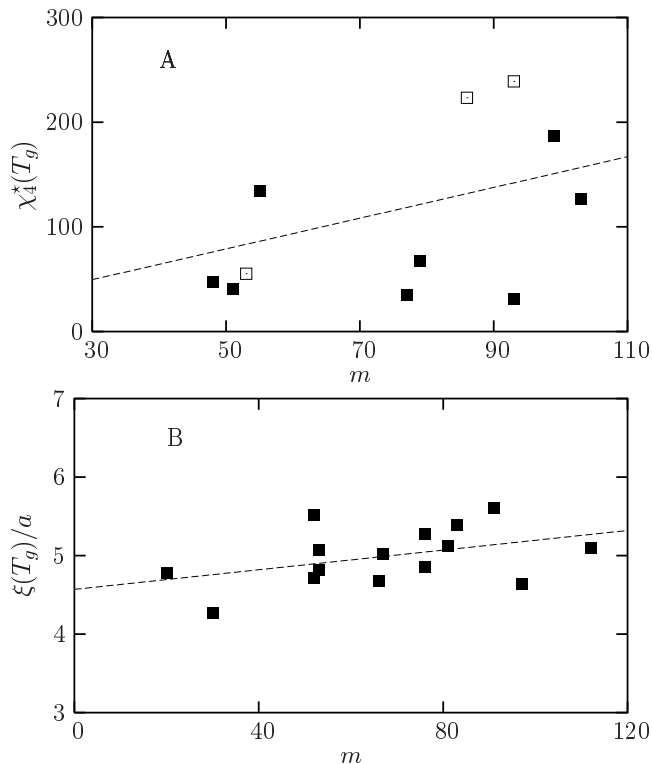
FIG. 2: (A) Correlation volume $\chi_4^\star(T_g)$ in supercooled liquids at the glass transition. Filled squares represent a lower bound to $\chi_4^\star(T_g)$ in molecular units estimated through Eq. 7. Different points represent different materials, which are ranked by their fragility m. Open squares represent the same quantity evaluated from available multidimensional NMR data, using [28] $\chi_4^\star = \int d^3r \exp(-2r/\xi)$, for glycerol ($T_g$+ 10 K) [27], orthoterphenyl (T_g + 9 K) [28, 34] and d-sorbitol (T_g+ 7 K) [28]. A linear fit to the weak increase of $\chi_4^\star$ with fragility is shown as a dashed line. (B) Correlation length $\xi(T_g)$ in supercooled liquids at the glass transition expressed in bead units a. The correlation volume is first evaluated using Δc_P instead of c_P in Eq. 7. Following [30], Δc_P is expressed in k_B "per bead" units accounting for different molecular shapes and sizes. Using $\zeta = 3$, the result is finally converted into a length scale expressed in bead units. The known empirical correlations [29] between m, β and Δc_P translate into a weak increase of $\xi(T_g)$ with fragility, which we fit with a linear relation shown as a dashed line.

appearing in Eq. 7 and assuming a stretched exponential form for $\mathcal{F}(x) = \exp(-x^\beta)$, we estimate $\chi_4^\star(T_g)$ for different glass-forming liquids in Fig. 2A.

For complex molecules, fluctuations that are unrelated to the glassy dynamics might contribute to the specific heat. These effects may be taken into account by replacing c_P in Eq. 7 by Δc_P, the jump in specific heat at T_g, which is sensitive only to the glassy degrees of freedom. Furthermore, for large molecules, the molecular size is probably not the relevant microscopic lengthscale, and it is sensible to express the specific heat in units of k_B per "independent bead" instead of molecular units [30]. These physical assumptions are used in Fig. 2B, where we have converted our results into lengthscales expressed in bead units, and they lead to a trend similar to that of the main plot but with less scatter: Dynamic correlations revealed by χ_T increase weakly with fragility [31]. This result is compatible with some theoretical approach [32], but contrasts with others that predict an opposite trend [33]. This discrepancy might arise from the existence of at least two physically distinct dynamic lengthscales, one revealed by χ_T, and a second associated to χ_4. Although we found that both quantities are comparable for fragile systems, the bound in relation 5 may underestimate χ_4 for strong materials.

To further test our length scale estimate of Eq. 7, we apply the formula to a polymeric liquid poly(vinyl acetate) (PVAc) using the monomer size for a [27]. We find $\xi \approx 2.0$ nm at T_g, to be compared with the value of 3.7 ± 1 nm obtained at T_g+10K [9, 28] [we assume $\zeta = 3$, and use the data on PVAc given in [9, 28]]. Again, the agreement is satisfactory. A similar agreement is found for orthoterphenyl and sorbitol, for which available NMR data are reported in Fig. 2A. Hence, we find that typical values for the dynamic correlation length at T_g obtained via Eq. 7 are in good agreement with previous experiments performed near T_g [1, 8, 9, 27, 34]. However, our approach has a broader scope, because it allows one to extend experimental studies of dynamic heterogeneity to a range of temperatures not previously accessible and to the full time dependence of the fluctuations (Fig. 1). Finally, we remark that even for (strong) Arrhenius molecular liquids with activation energy E, relation 5 and time temperature superposition give $\chi_4^\star(T) \geq (k_B/c_P) \times E^2/(k_BT)^2$, showing that dynamic heterogeneity must also exist in that case [35], in agreement with the general argument that for systems with finite range interactions, diverging time scales must be accompanied by diverging length scales.

Our experiments provide a quantitative demonstration that dynamic correlations and length scales increase as the glass transition is approached. More work is needed to characterize the time and temperature dependencies of dynamic fluctuations over a larger range of materials and parameters. Open issues also concern the precise space-time geometry of dynamic heterogeneity that fixes the value of the exponent ζ and the relation between time scales and length scales, the connection between cooperativity and heterogeneity, and the extension of our results to the nonequilibrium aging dynamics encountered in the glass phase.

[1] E. Donth, *The glass transition* (Springer, Berlin, 2001).

[2] P.G. Debenedetti and F.H. Stillinger, *Nature* **410**, 259

(2001).

[3] M.M. Hurley and P. Harrowell, *Phys. Rev. E* **52**, 1694 (1995).

[4] C. Bennemann, C. Donati, J. Baschnagel, and S.C. Glotzer, *Nature* **399**, 246 (1999).

[5] C. Donati, S. Franz, S.C. Glotzer, G. Parisi, *J. Non-Cryst. Solids* **307-310**, 215 (2002).

[6] S. Whitelam, L. Berthier, J.P. Garrahan, *Phys. Rev. Lett.* **92**, 185705 (2004).

[7] L. Berthier, *Phys. Rev. E* **69**, 020201 (2004).

[8] M.D. Ediger, *Annu. Rev. Phys. Chem.* **51**, 99 (2000).

[9] U. Tracht, *et al.*, *Phys. Rev. Lett.* **81**, 2727 (1998).

[10] E. Weeks, J.C. Crocker, A.C. Levitt, A. Schofield, D.A. Weitz, *Science* **287**, 627 (2000).

[11] E. Vidal-Russell and N.E. Israeloff, *Nature* **408**, 695 (2000).

[12] L.A. Deschenes and D.A. Vanden Bout, *Science* **292**, 255 (2001).

[13] T.R. Kirkpatrick, D. Thirumalai, and P.G. Wolynes, *Phys. Rev. A* **40**, 1045 (1989).

[14] P. Viot., G. Tarjus, and D. Kivelson, *J. Chem. Phys.* **112**, 10368 (2000).

[15] J.P. Garrahan and D. Chandler, *Phys. Rev. Lett.* **89**, 035704 (2002).

[16] C. Toninelli, M. Wyart, G. Biroli, L. Berthier, and J.P. Bouchaud, *Phys. Rev. E* **71**, 041505 (2005).

[17] P. Mayer *et al.*, *Phys. Rev. Lett.* **93**, 115701 (2004).

[18] G. Tarjus, D. Kivelson, S. Mossa, and C. Alba-Simionesco, *J. Chem. Phys.* **120**, 6135 (2004).

[19] P.N. Pusey and W. van Megen, *Nature* **320**, 340 (1986).

[20] J.P. Hansen and I.R. Mc Donald, *Theory of simple liquids* (Elsevier, Amsterdam, 1986).

[21] J.L. Lebowitz, J.K. Percus, and L. Verlet, *Phys. Rev.* **153**, 250 (1967).

[22] Alternatively, this inequality may be derived from standard probability theory. From the Cauchy-Schwarz inequality one obtains that the average $k_B T^2 \chi_T(t)/N = \langle \delta C(t) \delta H(0) \rangle$ is $\leq [\langle \delta C(t) \delta C(t) \rangle \langle \delta H(0) \delta H(0) \rangle]^{1/2}$. Using the fluctuation-dissipation relation to express enthalpy fluctuation in terms of the specific heat at constant pressure, one directly obtains relation 5. Contrary to the derivation in the main text, this argument does not provide any estimate of the difference between the two sides of the relation 5.

[23] D. El Masri, M. Pierno, L. Berthier, and L. Cipelletti, *J. Phys. Condens. Matter* **17** S3543 (2005).

[24] W. Kob and H.C. Andersen, *Phys. Rev. Lett.* **73**, 1376 (1994).

[25] The numerical model is a 80:20 binary Lennard-Jones mixture at density $\rho = 1.2$. A and B particles interact via a Lennard-Jones potential $V(\mathbf{r}_{\alpha\beta}) = 4\epsilon_{\alpha\beta} \left[(\sigma_{\alpha\beta}/r_{\alpha\beta})^{12} - (\sigma_{\alpha\beta}/r_{\alpha\beta})^6 \right]$, with $\alpha, \beta = A, B$. Time, energy and length are measured in units of σ_{AA} and ϵ_{AA}, and $\sqrt{m_A \sigma_{AA}^2 / \epsilon_{AA}}$, respectively. Other parameters are $\epsilon_{AB} = 1.5$, $\epsilon_{BB} = 0.5$, $\sigma_{BB} = 0.88$, $\sigma_{AB} = 0.8$. Newton equations are integrated using a velocity Verlet algorithm with time step 0.01. Characteristic temperatures for this system are the onset of slow dynamics, $T_o \approx 1.0$, and $T_c \approx 0.435$, the location of the mode-coupling singularity in the analysis of Kob and Andersen [24].

[26] G. Biroli and J.P. Bouchaud, *Europhys. Lett.* **67**, 21 (2004).

[27] S.A. Reinsberg, X.H. Qiu, M. Wilhelm, H.W. Spiess, and M.D. Ediger, *J. Chem. Phys.* **114**, 7299 (2001).

[28] X.H. Qiu and M.D. Ediger, *J. Phys. Chem. B* **107**, 459 (2003).

[29] L.M. Wang, V. Velikov, and C.A. Angell, *J. Chem. Phys.* **118** 10184 (2003).

[30] J.D. Stevenson and P.G. Wolynes, *J. Phys. Chem. B* **109**, 15093 (2005).

[31] A similar correlation is discussed in [36].

[32] X.Y. Xia and P.G. Wolynes, *Proc. Natl. Acad. Sci.* **97**, 2990 (2000).

[33] J.P. Garrahan and D. Chandler, *Proc. Natl. Acad. Sci.* **100**, 9710 (2003).

[34] S.A. Reinsberg, A. Heuer, B. Doliwa, H. Zimmermann, and H.W. Spiess, *J. Non-Cryst. Solids* **307-310**, 208 (2002).

[35] The energy conservation is central to this argument which does not apply, for instance, to Langevin dynamics where the thermal bath can locally provide energy to the system. In this case, no growing dynamic length is expected in Arrhenius liquids.

[36] E. Hempel, G. Hempel, A. Hensel, C. Schick, and E. Donth, *J. Phys. Chem. B* **104**, 2460 (2000).

[37] We thank A. Schofield for providing us with the colloidal particles. L.C. is a junior member of the Institut Universitaire de France. M.P. is supported by the MCRTN Arrested Matter. This work was also supported by Centre National d'Etudes Spatiales, and the French ministère de la Recherche through an ACI Jeunes Chercheurs.